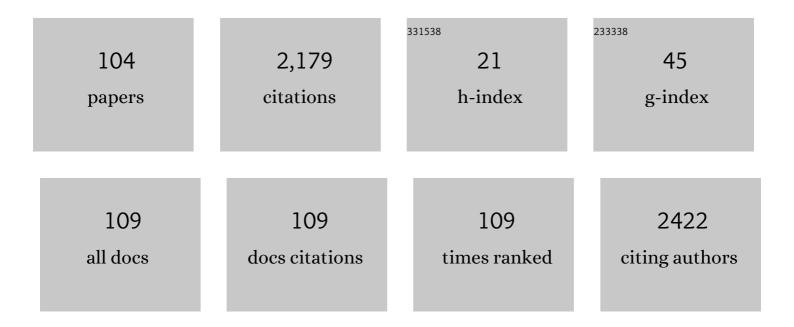
Hiroshi Shinmoto

List of Publications by Year in descending order

Source: https://exaly.com/author-pdf/4059057/publications.pdf Version: 2024-02-01



#	Article	IF	CITATIONS
1	Lower limb lymphedema staging based on magnetic resonance lymphangiography. Journal of Vascular Surgery: Venous and Lymphatic Disorders, 2022, 10, 445-453.e3.	0.9	6
2	Membranous urethral length on magnetic resonance imaging as a novel predictor of urinary continence after delayed anastomotic urethroplasty for pelvic fracture urethral injury. World Journal of Urology, 2022, 40, 147-153.	1.2	2
3	Combining the Tumor Contact Length and Apparent Diffusion Coefficient Better Predicts Extraprostatic Extension of Prostate Cancer with Capsular Abutment: A 3 Tesla MR Imaging Study. Magnetic Resonance in Medical Sciences, 2022, 21, 477-484.	1.1	2
4	Assessment of pulmonary arteriovenous malformation with ultra-short echo time magnetic resonance imaging. European Journal of Radiology, 2022, 147, 110144.	1.2	4
5	Role of magnetic resonance imaging in the management of male pelvic fracture urethral injury. International Journal of Urology, 2022, 29, 919-929.	0.5	6
6	Magnetic resonance imaging findings of pure prostatic ductal adenocarcinomas: a case series. Abdominal Radiology, 2022, 47, 1929-1938.	1.0	1
7	Treatment of massive hemoptysis after thoracic aortic aneurysm repair. CVIR Endovascular, 2022, 5, 17.	0.4	0
8	MRIâ€detectability and histological factors of prostate cancer including intraductal carcinoma and cribriform pattern. Prostate, 2022, 82, 452-463.	1.2	7
9	Successful Treatment of Subcapsular Hepatic Hemorrhage Concomitant with Diffuse Arterioportal Shunt by Transcatheter Arterial Embolization. Interventional Radiology, 2022, , .	0.2	0
10	Effect of Ultra-High-Resolution CT on Pseudoenhancement in Renal Cysts: A Phantom Experiment and Clinical Study. American Journal of Roentgenology, 2022, 219, 624-633.	1.0	2
11	Magnetic Resonance Lymphangiography Staging System for Lower Limb Lymphedema [Presidential Award Proceedings]. Japanese Journal of Magnetic Resonance in Medicine, 2022, 42, 53-57.	0.0	0
12	Composite pheochromocytoma–ganglioneuroma: a case with two distinct components radiographically. BJR case Reports, 2022, 8, .	0.1	0
13	Successful Closure of External Iliac Artery Perforation with Super-selective Transcatheter Coil Embolization. Interventional Radiology, 2022, 7, 75-80.	0.2	0
14	MR Imaging of Hair and Scalp for the Evaluation of Androgenetic Alopecia. Magnetic Resonance in Medical Sciences, 2021, 20, 160-165.	1.1	3
15	Analysis of collateral lymphatic circulation in patients with lower limb lymphedema using magnetic resonance lymphangiography. Journal of Vascular Surgery: Venous and Lymphatic Disorders, 2021, 9, 471-481.e1.	0.9	8
16	Quantitative analysis of the anatomical changes in the scalp and hair follicles in androgenetic alopecia using magnetic resonance imaging. Skin Research and Technology, 2021, 27, 56-61.	0.8	6
17	Postoperative pneumonia causes the loss of skeletal muscle volume and poor prognosis in patients undergoing esophagectomy for esophageal cancer. General Thoracic and Cardiovascular Surgery, 2021, 69, 84-90.	0.4	13
18	T1ϕmagnetic resonance imaging value as a potential marker to assess the severity of liver fibrosis: A pilot study. European Journal of Radiology Open, 2021, 8, 100321.	0.7	3

#	Article	IF	CITATIONS
19	Mild metatropic dysplasia: emphasis on the magnetic resonance imaging of articular cartilage thickening. BJR case Reports, 2021, 7, 20200155.	0.1	0
20	Usefulness of computed tomography for hospitalized adult patients with fever to investigate cause of fever: single-center, retrospective cohort study. Japanese Journal of Radiology, 2021, 39, 802-810.	1.0	0
21	Diffuse Alveolar Hemorrhage Associated with Dilated Cardiomyopathy and Sleep Apnea Syndrome. Internal Medicine, 2021, 60, 1911-1914.	0.3	0
22	Laryngeal schwannoma with extralaryngeal extension mimicking a thyroid tumour. BJR case Reports, 2021, 7, 20210089.	0.1	2
23	Angioleiomyoma of the extremities: correlation of magnetic resonance imaging with histopathological findings in 25 cases. Skeletal Radiology, 2021, , 1.	1.2	4
24	Applicability of ultrasonography for detection of marginal sinus placenta previa. Medicine (United) Tj ETQq0 0 0	rgBT /Over 0.4	·lo _၄ k 10 Tf 50
25	Ultra-short echo time magnetic resonance angiography using a modified signal targeting with alternative radio frequency spin labeling technique for detecting recanalized pulmonary arteriovenous malformation after coil embolization. Acta Radiologica Open, 2021, 10, 205846012110576.	0.3	2
26	Analysis of Diffusion-weighted MR Images Based on a Gamma Distribution Model to Differentiate Prostate Cancers with Different Gleason Score. Magnetic Resonance in Medical Sciences, 2020, 19, 40-47.	1.1	4
27	Double Balloon-Occluded Transarterial Chemoembolization (Double B-TACE) for Hepatocellular Carcinomas Located in the Caudate Lobe. CardioVascular and Interventional Radiology, 2020, 43, 162-164.	0.9	5
28	Magnetic Resonance Imaging Findings of Traumatic Bulbar Urethral Stricture Help Estimate Repair Complexity. Urology, 2020, 135, 146-153.	0.5	3
29	COVID â€19 in older adults: Retrospective cohort study in a tertiary hospital in Japan. Geriatrics and Gerontology International, 2020, 20, 1044-1049.	0.7	5
30	Repeat Balloon-Occluded Retrograde Transvenous Obliteration for Recurrent Gastric Varices via the Left Inferior Phrenic Vein. Journal of Vascular and Interventional Radiology, 2020, 31, 1914-1916.e1.	0.2	0
31	Prostate cancer recurrence mimicking invasive urothelial cancer of the bladder. Urology Case Reports, 2020, 33, 101421.	0.1	2
32	The use of magnetic resonance imaging to predict placenta previa with placenta accreta spectrum. Acta Obstetricia Et Gynecologica Scandinavica, 2020, 99, 1657-1665.	1.3	10
33	Balloon-occluded retrograde glue embolization for intractable lymphorrhea from bilateral iliac lymphatics following surgery for rectal cancer. Radiology Case Reports, 2020, 15, 371-374.	0.2	6
34	A rare case of isolated splenic sarcoidosis: A case report and literature review. Molecular and Clinical Oncology, 2020, 14, 22.	0.4	4
35	Acquired Cystic Disease-Associated Renal Cell Carcinoma Extending to the Renal Pelvis Mimicking Urothelial Carcinoma on Computed Tomography (CT): Two Case Reports. American Journal of Case Reports, 2020, 21, e926630.	0.3	1
36	Acquired Cystic Disease-Associated Renal Cell Carcinoma Extending to the Renal Pelvis Mimicking Urothelial Carcinoma on Computed Tomography (CT): Two Case Reports. American Journal of Case Reports, 2020, 21, e926630.	0.3	6

#	Article	IF	CITATIONS
37	Magnetic Resonance Imaging Findings of Penile Abscess. Urology, 2019, 131, e5-e6.	0.5	6
38	Histological differences in cancer cells, stroma, and luminal spaces strongly correlate with in vivo MRI-detectability of prostate cancer. Modern Pathology, 2019, 32, 1536-1543.	2.9	21
39	Restoration of Dehiscent Pancreaticojejunostomy Causing a Major Postoperative Pancreatic Fistula by Reinsertion of a Pancreatic Duct Tube Using the Rendezvous Technique. CardioVascular and Interventional Radiology, 2019, 42, 1358-1362.	0.9	2
40	Mobile Spinal Schwannoma with a Completely Cystic Appearance. American Journal of Case Reports, 2019, 20, 859-863.	0.3	10
41	A Case of Retroperitoneal Extrarenal Angiomyolipoma Associated with a Huge Hematoma and Coagulopathy. Nihon Rinsho Geka Gakkai Zasshi (Journal of Japan Surgical Association), 2019, 80, 2277-2283.	0.0	Ο
42	The added value of tomosynthesis in endoscopic retrograde cholangiography with radiography for the detection of choledocholithiasis. British Journal of Radiology, 2018, 91, 20180115.	1.0	0
43	Reply. Urology, 2018, 112, 204.	0.5	2
44	Pubourethral Stump Angle Measured on Preoperative Magnetic Resonance Imaging Predicts Urethroplasty Type for Pelvic Fracture Urethral Injury Repair. Urology, 2018, 112, 198-204.	0.5	21
45	Response to Correspondence: Marginal sinus placenta previa is a different entity in placenta previa: A retrospective study using magnetic resonance imaging. Taiwanese Journal of Obstetrics and Gynecology, 2018, 57, 910.	0.5	1
46	Bosniak Category III Renal Cysts Caused by Crizotinib in an Anaplastic Lymphoma Kinase Gene-Rearranged Non–Small Cell Lung Cancer Patient. Urology, 2018, 121, e3-e4.	0.5	5
47	Marginal sinus placenta previa is a different entity in placenta previa: A retrospective study using magnetic resonance imaging. Taiwanese Journal of Obstetrics and Gynecology, 2018, 57, 532-535.	0.5	14
48	Clinically mild encephalopathy with a reversible splenial lesion and nonconvulsive status epilepticus in a schizophrenic patient with neuroleptic malignant syndrome. Psychiatry and Clinical Neurosciences, 2017, 71, 212-212.	1.0	6
49	Possibility of transrectal photoacoustic imaging-guided biopsy for detection of prostate cancer. Proceedings of SPIE, 2017, , .	0.8	4
50	Clinical implication of ectopic liver lipid accumulation in renal cell carcinoma patients without visceral obesity. Scientific Reports, 2017, 7, 12795.	1.6	3
51	Blood-oxygen-level-dependent (BOLD) functional magnetic resonance imaging (fMRI) during transcranial near-infrared laser irradiation. Brain Stimulation, 2017, 10, 1136-1138.	0.7	6
52	Pilot Study of Prostate Cancer Angiogenesis Imaging Using a Photoacoustic Imaging System. Urology, 2017, 108, 212-219.	0.5	51
53	Clinical outcomes of percutaneous radiofrequency ablation for small renal cancer. Oncology Letters, 2017, 14, 918-924.	0.8	10
54	A Case of Hemorrhagic Adrenal Pseudocyst Mimicking Solid Tumor. American Journal of Case Reports, 2017, 18, 1034-1038.	0.3	6

#	Article	IF	CITATIONS
55	Removing Ambiguity Caused by T ₂ Shine-through using Weighted Diffusion Subtraction (WDS). Magnetic Resonance in Medical Sciences, 2016, 15, 146-148.	1.1	4
56	A pilot study of photoacoustic imaging system for improved realâ€ŧime visualization of neurovascular bundle during radical prostatectomy. Prostate, 2016, 76, 307-315.	1.2	53
57	Synchronous neuroendocrine tumors in both the pancreas and ileum: A case report. International Journal of Surgery Case Reports, 2016, 22, 47-50.	0.2	3
58	Role of computed tomography urography in the clinical evaluation of upper tract urothelial carcinoma. International Journal of Urology, 2016, 23, 284-298.	0.5	59
59	Comparison of transrectal photoacoustic, Doppler, and magnetic resonance imaging for prostate cancer detection. Proceedings of SPIE, 2016, , .	0.8	6
60	Diffusion-weighted MR Imaging for the Assessment of Renal Function: Analysis Using Statistical Models Based on Truncated Gaussian and Gamma Distributions. Magnetic Resonance in Medical Sciences, 2016, 15, 237-245.	1.1	9
61	Intrahepatic Cholangiocarcinoma With Lymphoepithelioma-like Carcinoma Components Not Associated With Epstein-Barr Virus: Report of a Case. International Surgery, 2015, 100, 689-695.	0.0	21
62	Transarterial embolization for pediatric hepatocellular carcinoma with cardiac cirrhosis. Pediatrics International, 2015, 57, 766-770.	0.2	28
63	Diffusion-weighted imaging of prostate cancer using a statistical model based on the gamma distribution. Journal of Magnetic Resonance Imaging, 2015, 42, 56-62.	1.9	13
64	Anterior Prostate Cancer: Diagnostic Performance of T2-Weighted MRI and an Apparent Diffusion Coefficient Map. American Journal of Roentgenology, 2015, 205, W185-W192.	1.0	12
65	Magnetic resonance enterocolonography in detecting erosion and redness in intestinal mucosa of patients with <scp>C</scp> rohn's disease. Journal of Gastroenterology and Hepatology (Australia), 2015, 30, 667-673.	1.4	26
66	Time Course of Osteonecrosis in Rabbit Articular Intercalated Bone: Line Scan Spectroscopic Imaging and Correlation with Histology. Magnetic Resonance in Medical Sciences, 2015, 14, 57-64.	1.1	2
67	Interpretation of Diffusion MR Imaging Data using a Gamma Distribution Model. Magnetic Resonance in Medical Sciences, 2014, 13, 191-195.	1.1	21
68	Diffusion kurtosis imaging study of prostate cancer: Preliminary findings. Journal of Magnetic Resonance Imaging, 2014, 40, 723-729.	1.9	93
69	18F-FDG PET/CT and MR Findings of Ovarian Carcinoid Within a Dermoid Cyst. Clinical Nuclear Medicine, 2014, 39, e392-e394.	0.7	4
70	Right-sided retrocaval approach using guidance via the lesser sac for Spieghel lobe resection. Surgery, 2013, 153, 282-286.	1.0	1
71	Superparamagnetic iron oxide-enhanced interstitial magnetic resonance lymphography to detect a sentinel lymph node in tongue cancer patients. Acta Oto-Laryngologica, 2013, 133, 418-423.	0.3	18
72	Laparoscopic Enucleation of Macronodules in a Patient with ACTH-Independent Macronodular Adrenal Hyperplasia 7 Years after Unilateral Adrenalectomy: Consideration of Operative Procedure. Urologia Internationalis, 2013, 90, 253-258.	0.6	7

#	Article	IF	CITATIONS
73	An Intravoxel Incoherent Motion Diffusion-Weighted Imaging Study of Prostate Cancer. American Journal of Roentgenology, 2012, 199, W496-W500.	1.0	95
74	Multiple atypical polypoid adenomyoma of the uterus. Japanese Journal of Radiology, 2012, 30, 606-611.	1.0	4
75	Comparison of animal studies between interstitial magnetic resonance lymphography and radiocolloid SPECT/CT lymphoscintigraphy in the head and neck region. Annals of Nuclear Medicine, 2012, 26, 281-285.	1.2	6
76	Importance of Maintaining Left Gastric Arterial Flow at Appleby Operation Preserving Whole Stomach for Central Pancreatic Cancer. Hepato-Gastroenterology, 2012, 59, 2650-2.	0.5	8
77	Comparison of T2-weighted and contrast-enhanced T1-weighted MR imaging at 1.5ÅT for assessing the local extent of cervical carcinoma. European Radiology, 2011, 21, 1850-1857.	2.3	29
78	Prospective study of combination therapy with low-dose thalidomide plus prednisolone ameliorating cytopenia in primary myelofibrosis. International Journal of Hematology, 2011, 93, 129-131.	0.7	3
79	Pneumonia induced by swine-origin influenza A (H1N1) infection: chest computed tomography findings in children. Japanese Journal of Radiology, 2011, 29, 712-7.	1.0	9
80	lgC4-associated Multifocal Systemic Fibrosis Detected by Cancer Screening with 18F-FDG Positron Emission Tomography/Computed Tomography. Radioisotopes, 2010, 59, 173-177.	0.1	0
81	Biexponential apparent diffusion coefficients in prostate cancer. Magnetic Resonance Imaging, 2009, 27, 355-359.	1.0	97
82	A Comparative Study of Spinal Bone SPECT versus X-ray Radiograph, CT or MRI in Patients with an Acute Compression Fracture of a Thoracolumbar Vertebral Body. Radioisotopes, 2009, 58, 719-726.	0.1	1
83	18F-FDC-PET/CT as an indicator for resection of pulmonary epithelioid hemangioendothelioma. Annals of Nuclear Medicine, 2008, 22, 521-524.	1.2	43
84	Semiquantitative Assessment of MR Imaging in Prediction of Efficacy of Gonadotropin-releasing Hormone Agonist for Volume Reduction of Uterine Leiomyoma: Initial Experience. Radiology, 2008, 248, 917-924.	3.6	10
85	Detection of Bladder Tumors with Dynamic Contrast-Enhanced MDCT. American Journal of Roentgenology, 2007, 188, 913-918.	1.0	48
86	Prostate cancer screening: The clinical value of diffusion-weighted imaging and dynamic MR imaging in combination with T2-weighted imaging. Journal of Magnetic Resonance Imaging, 2007, 25, 146-152.	1.9	319
87	The mechanism of ring enhancement in hepatocellular carcinoma on superparamagnetic iron oxide-enhanced T1-weighted images: An investigation into peritumoral Kupffer cells. Journal of Magnetic Resonance Imaging, 2005, 21, 230-236.	1.9	9
88	Superparamagnetic iron oxide-enhanced MR imaging for focal hepatic lesions: a comparison with CT during arterioportography plus CT during hepatic arteriography. Journal of Gastroenterology, 2005, 40, 371-380.	2.3	26
89	Angiomyolipomas That Do Not Contain Fat Attenuation at Unenhanced CT. Radiology, 2005, 234, 311-312.	3.6	22
90	Evaluation of ischemic heart disease on a 1.5 Tesla scanner: combined first-pass perfusion and viability study. Radiation Medicine, 2005, 23, 230-5.	0.8	12

#	Article	IF	CITATIONS
91	Successful pregnancy and normal delivery after whole craniospinal irradiation in two patients. Anticancer Research, 2005, 25, 3481-7.	0.5	2
92	Questionnaire survey of acute and delayed adverse reactions to ferumoxides. Radiation Medicine, 2005, 23, 468-73.	0.8	2
93	Pulmonary Hypoplasia: Prediction with Use of Ratio of MR Imaging–measured Fetal Lung Volume to US-estimated Fetal Body Weight. Radiology, 2004, 232, 767-772.	3.6	64
94	Massive hepatic infarction in preeclampsia: successful treatment with continuous hemodiafiltration and corticosteroid therapy. Journal of Perinatal Medicine, 2004, 32, 453-5.	0.6	4
95	KUPFFER CELL FUNCTION OF HEPATOCELLULAR ADENOMA: PULSE SEQUENCE EFFECTS IN SUPERPARAMAGNETIC IRON OXIDE-ENHANCED MAGNETIC RESONANCE IMAGING. Journal of Gastroenterology and Hepatology (Australia), 2004, 19, 951-952.	1.4	3
96	MRI of fetal abdominal abnormalities. Abdominal Imaging, 2003, 28, 877-86.	2.0	49
97	Superparamagnetic Iron Oxide–mediated Hepatic Signal Intensity Change in Patients with and without Cirrhosis: Pulse Sequence Effects and Kupffer Cell Function. Radiology, 2002, 222, 661-666.	3.6	80
98	Prenatal diagnosis of atelosteogenesis type I at 21 weeks' gestation. Prenatal Diagnosis, 2002, 22, 1071-1075.	1.1	20
99	Routine MR imaging protocol with breath-hold fast scans: diagnostic efficacy for focal liver lesions. Radiation Medicine, 2002, 20, 169-79.	0.8	5
100	MR Imaging of Non-CNS Fetal Abnormalities: A Pictorial Essay. Radiographics, 2000, 20, 1227-1243.	1.4	127
101	Virtual Laryngoscopy. Annals of Otology, Rhinology and Laryngology, 1999, 108, 221-226.	0.6	44
102	Small renal cell carcinoma: MRI with pathologic correlation. Journal of Magnetic Resonance Imaging, 1998, 8, 690-694.	1.9	73
103	Angiomyolipoma: imaging findings in lesions with minimal fat Radiology, 1997, 205, 497-502.	3.6	286
104	MR Appearance and Spectral Features of Injected Ethanol in the Liver: Implication for Fast MR-Guided Percutaneous Ethanol Injection Therapy. Journal of Computer Assisted Tomography, 1997, 21, 82-88.	0.5	12